4

Minimization of Losses in Converter-Fed Induction Motors – Optimal Flux Solution

Waldiberto de Lima Pires, Hugo Gustavo Gomez Mello,
Sebastião Lauro Nau and Alexandre Postól Sobrinho
WEG Equipamentos Eletricos S.A. – Motores
Research and Development of Product Department
Av. Pref. Waldemar Grubba, 3000 – malote 41
Jaraguá do Sul, SC - 89256-900
Brazil

1. Introduction

When a TEFC induction motor fed by static frequency converter drives a load which demands constant torque throughout the operation range, the low speeds are thermally critical, because the motor losses (heat sources) do not vary much as a function of the speed, but the ventilation efficiency decreases as the operation speed falls down, since the fan is installed on the very motor shaft. In such cases, when operating at low speeds, the temperature rise often exceeds the limits of the motor thermal class due to the lack of cooling. In order to prevent this problem the industry has traditionally adopted one of the following solutions: independent ventilation (a small auxiliary motor is used to exclusively drive the fan that provides the main motor cooling) or oversizing (the motor used in the application provides a higher torque than the rated load demand). However, neither one nor the other of these two options are attractive, as both, besides increasing the space required for the installation, still increase the motor price [1].
Frequency converters usually apply to the motor a constant voltage/frequency ratio throughout the operation range, so that no loss control is provided. But the study on the motor losses composition and its relation with voltage, frequency, magnetic flux and current, allied with the study on the influence of the ventilation on the temperature rise of the motor, has led to an optimal voltage/frequency ratio, which minimizes the total motor losses at each speed [2]. This way, by implementing the automatic control of the voltage/frequency ratio in the converter, the motor loss minimization can be automatically obtained throughout the frequency range, so that the motor temperature rise is kept within the thermal class limits even at low speeds with reduced ventilation.

2. Determination of losses

The fast growth of the number of industrial applications using static frequency converters recently observed in variable speed drives has encouraged the meticulous study of losses in magnetic materials under PWM supply by several researchers [3, 4, 5, 6, 7, 8]. They have

shown that such losses depend on a number of control parameters, such as the modulation index, the number of levels and pulses of the frequency converter and the duration of PWM signal pulses. On the other hand, Boglietti et alli have concluded that the flux waveforms resulting from PWM supply differ from those resulting from sinusoidal supply just except for a small ripple, which depends on the switching frequency, and that above approximately 5 kHz the iron losses can be considered independent of this parameter [9]. Such studies represent the first step towards the understanding of the losses behavior in electric motors under PWM supply, that involves a higher degree of complexity and is not restricted exclusively to the magnetic materials issue, but includes also additional losses in the conductors and due to the cooling system and depends, besides the control parameters, on some machine design parameters, such as the flux density, the lamination geometry and the connection of windings [3, 10, 11, 12], as well as on other variables inherent to the manufacturing process [13].

For the purposes of this study, however, the analysis of the motor losses can be simplified, so that it is enough to separate the total motor losses in three key components:

$$P = Pfe + Pj + Pmec \tag{1}$$

where:

Pfe – Iron losses, which depend on the flux density (or magnetic induction), the frequency and the quality of the magnetic material.

Pj – Losses by Joule effect, which depend on the currents flowing through the stator windings and the rotor bars.

Pmec – Mechanical losses due to cooling system (fan coupled to the shaft) and friction, which depend on the speed.

The iron losses are classically considered as being composed of two portions: Hysteresis losses (pH) and induced eddy current (Foucault) losses (pF). For a lamination sample tested in Epstein Frame with sinusoidal supply, the hysteresis losses are directly proportional to the frequency (f) and to the square of the magnetic induction (B^2), while the eddy current losses are proportional to the square of both the frequency (f^2) and the magnetic induction (B^2), especially for induction values above one Tesla (1 T). However, in the induction motor the iron losses present a much more induction-dependent behavior than the quadratic ratio obtained with normalized samples of the magnetic material in Epstein Frame tests. In low-voltage three-phase induction motors manufactured with fully processed steel laminations tested under different saturation levels, iron losses presented a dependance on the induction close to B^4 for inductions above 1,2 T (usual value for industrial motors), as presented in Fig. 1.

The fundamental theory of the electric machines shows that the torque provided by the induction motor is directly proportional to the product between the magnetic flux and the electric current [14, 15]. Then in order to keep a constant torque, if the flux increases the current can decrease (and vice-versa). As the Joule losses are directly proportional to the square of the current, these losses can be considered as inversely proportional to the square of the magnetic flux. From the Faraday-Lenz law of induction, one can easily demonstrate that the magnetic flux in the motor is directly proportional to the ratio between the electromotive force (E) and the frequency. Considering the steady-state model of equivalent circuit of the induction motor per-phase (Fig. 2), it can be noted that at the base frequency the voltage drop in the primary impedance has little significance, so that the flux can be considered as proportional to the *V1/f* (voltage/frequency) ratio.

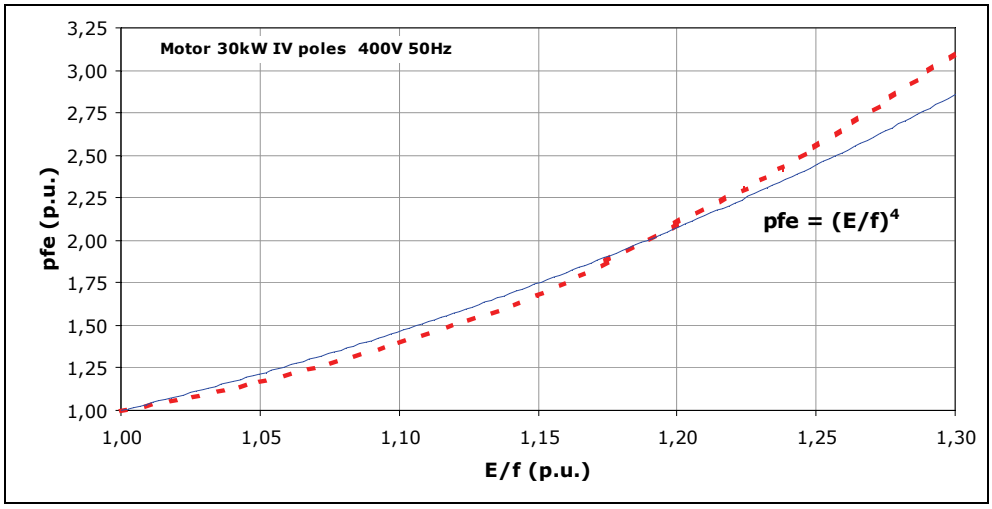

Fig. 1. Iron losses x Magnetic induction for an industrial three-phase induction motor

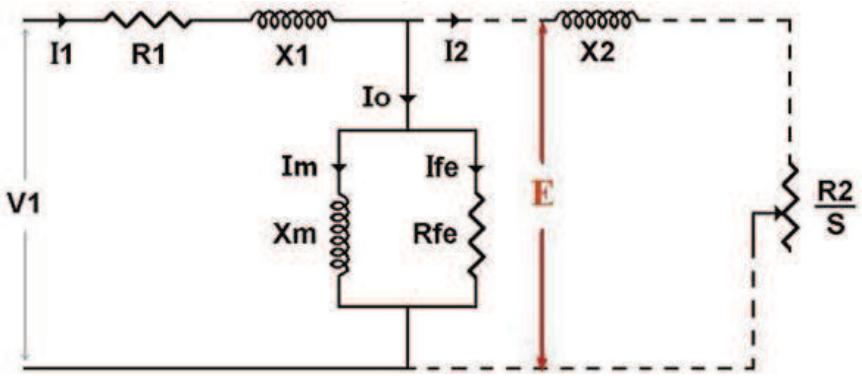

Fig. 2. Steady state equivalent circuit of the induction motor per-phase

For low operating frequencies, however, in which the input voltage is reduced, the voltage drop in the primary resistance becomes important and can be no longer despised. By neglecting the influence of the primary reactance, electromotive force E is given by

$$E = V - R_1 I_1 = V - \Delta V \tag{2}$$

The voltage drop at the stator branch (ΔV) then depends directly on the stator current ($I1$). As Fig. 2 shows, the motor current can be decomposed into two components: one concerning magnetization and the other concerning torque production.

$$I_1 = \sqrt{I_0^{\,2} + I_2^{\,2}} \tag{3}$$

Taking rated voltage as the base, *E/f* ratio per unit can be written as:

$$\frac{E}{f} = \frac{V}{f} - \frac{\Delta V_n}{f}\sqrt{\frac{k_T^{\,2}.k_m^{\,2}}{\left(\frac{E}{f}\right)^2} + k_{i0n}^{\,2}.k_{i0}^{\,2}} \tag{4}$$

where:
ΔVn - Voltage drop per unit with rated frequency and load.
f – Motor operating frequency per unit, considering rated frequency fn as the base.
In (4), the square root results in a correction factor, which is function of the motor current and whose terms are explained in the following paragraphs.
It should be taken into account that, as the frequency (and consequently, the rotation) is reduced, the mechanical losses decrease in a nearly cubic proportion to it (f^3). The mechanical losses do not affect the iron losses, but they act as an additional load to the motor, therefore they must be considered as a torque to be added to the rated torque available on the shaft. Its reduction implies current reduction and so reduction of Joule losses in the conductors (Pj).
Thus it is possible to rewrite the induction motor total losses per unit p, for operation with variable voltage and frequency, as follows:

$$p = p_{in}\left[\frac{k_T^{\,2}.k_m^{\,2}}{\left(\frac{E}{f}\right)^2} + k_{i0n}^{\,2}.k_{i0}^{\,2}\right] + p_{Hn}\left(\frac{E}{f}\right)^4 f + p_{Fn}\left(\frac{E}{f}\right)^4 f^2 \tag{5}$$

where:
pin – Total Joule losses with the motor operating at rated conditions of load, voltage and frequency.
pHn – Total hysteresis losses with the motor operating at rated conditions of load, voltage and frequency.
pFn – Total eddy current losses with the motor operating at rated conditions of load, voltage and frequency.
Motors manufactured with low loss magnetic core (fully processed silicon steel) operating at rated conditions typically present values of 80%, 12% and 8%, for parameters pin, pHn and pFn, respectively. The remaining parameters of (5) will be opportunely explained ahead.
The term of (5) in brackets refers to the motor Joule losses and depends on the total motor current. The second and third terms refer to the motor iron losses for hysteresis and eddy currents, respectively. The magnetic induction was conveniently replaced by the E/f ratio. There is no explicit term for the motor total mechanical losses in the equation, because they are embedded in the first term, in accordance with what was mentioned before, by means of the factor km defined below:

$$k_m = \left(\frac{1 + p_{mn} f^3}{1 + p_{mn}}\right) \tag{6}$$

where pmn is the mechanical losses at rated speed referred to the rated output power Pn.
The aim of this study is to minimize the motor losses, in order to reduce its temperature rise, so that the need of both the torque reduction (oversizing) and the use of independent ventilation can be prevented. In (5), this is considered by means of the derating factor kT,

which will be addressed later on this paper. It should be noted that the torque affects only the current-dependent losses, not influencing the iron losses. Therefore, *km* and *kT* are torque correction factors required to compensate for the effects of the speed variation, which influences the portion of losses related to the load current.
Ki0n is the no-load current factor, defined by (7).

$$k_{i0n} = \frac{I_o}{I_n} \tag{7}$$

where:
Io – No-load current under rated voltage and frequency.
In – Full-load current under rated voltage and frequency.
Due to the non-linearity of the magnetization curve of the laminations, the *E/f* ratio increase causes the no-load current to increase according to (8). This peculiar behavior of the no-load current was observed experimentally (Fig. 3), and is taken into account in (5) by means of the factor *ki0*.

$$k_{i0} = \left(\frac{E}{f}\right)^{3,4} \; para \;\; \frac{E}{f} \geq 1$$
$$k_{i0} = \left(\frac{E}{f}\right) \; para \;\; \frac{E}{f} < 1 \tag{8}$$

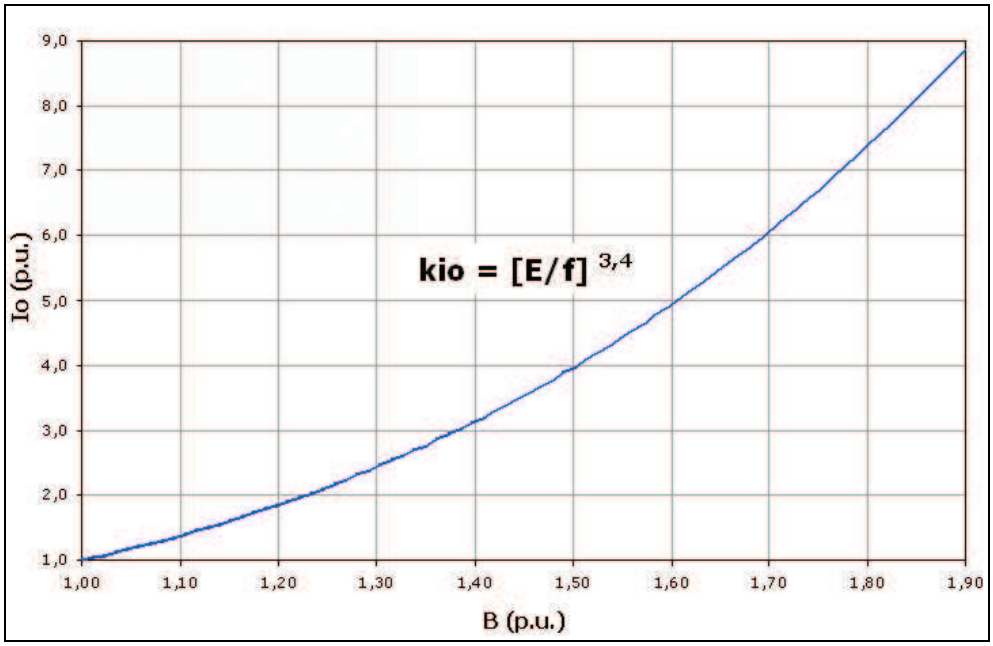

Fig. 3. Magnetizing current x E/f

3. Minimization of losses

The analysis of (5) shows that the induction motor global losses depend on both the operation frequency and the induction (or magnetic flux). Then the values of *V/f* that minimize the motor global losses change with the operation frequency, so that it is necessary to find the minimum losses at each frequency, with different values of *V/f*. Fig. 4 shows the total losses calculated as function of the frequency for various values of the *V/f* ratio.

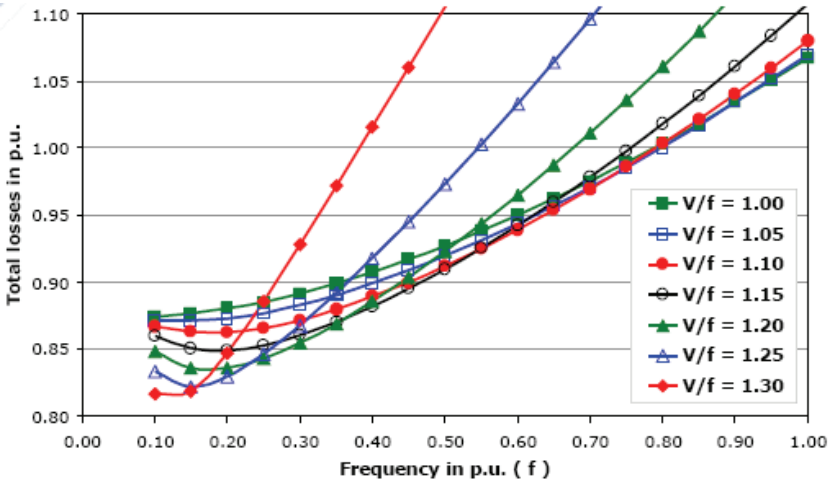

Fig. 4. Total losses x frequency curve for several V/f ratios at rated torque

Fig. 5 derives from the family of curves above and represents the V/f ratios theoretically obtained, which minimize the total losses of the motor at each operation frequency.

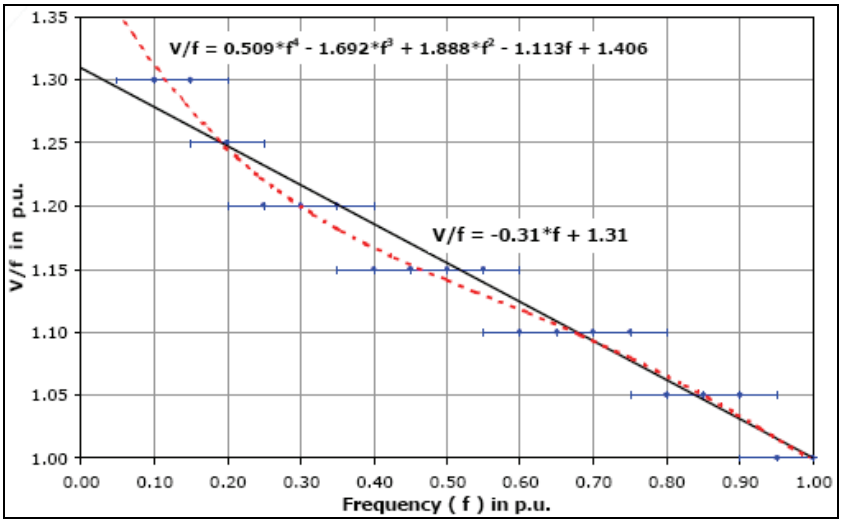

Fig. 5. V/f x frequency curve for minimization of total losses

4. Influence of ventilation reduction

Thermal calculations implemented for a number of motors of distinct frame sizes and power ratings considering speed variation, combined with experiments and tests performed with several motors at rated load, varying separately the fan speed from zero to base speed, led to the conclusion that TEFC three-phase motors of a wide output range present a similar thermal behavior. Fig. 6 represents the temperature rise per unit of low-voltage 4-pole cage induction motors manufactured with die cast iron frame as a function of the fan speed per unit.

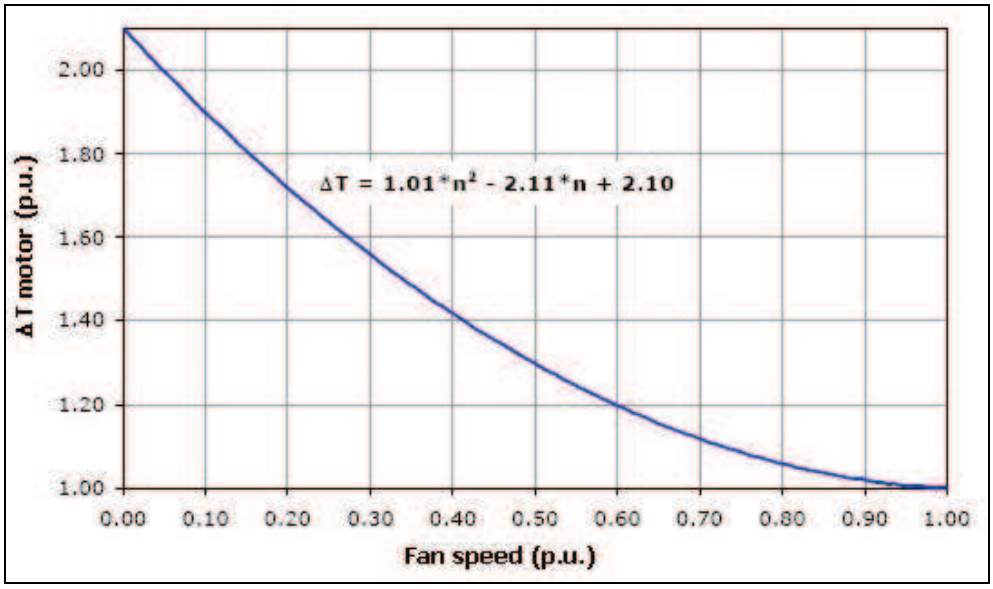

Fig. 6. Temperature rise x fan speed at rated load

In this approach, for each desired value of frequency and for each value of *V/f* ratio according to Fig. 5, the total losses *p* are calculated according to (5). Fig. 6 determines the influence of the ventilation reduction on the motor temperature rise (ΔT_{motor}). So in order for the required motor temperature rise to be assured, it is necessary to calculate a new value of *p*, henceforth referred to as *p'*, according to (9).

$$p' = \left(\frac{\Delta T}{\Delta T_{motor}} \right) p_n \tag{9}$$

where:

p' – total motor losses for the required temperature rise, considering the ventilation reduction.

pn - total motor losses at rated conditions.

If, for instance, the maximum required temperature rise is the limit of the insulation system thermal class, then $\Delta T = \Delta T_{class}$. If, otherwise, the maximum required temperature rise is ΔTn, then $\Delta T=1$.

Once known the total losses p' that will cause the required temperature rise in the motor with reduced ventilation, then it is possible to calculate the convenient derating factor using (10):

$$k_T = \frac{k_{HVF}}{k_m}\left(\frac{E}{f}\right)\sqrt{\frac{p' - p_{Hn}\left(\frac{E}{f}\right)^4 f - p_{Fn}\left(\frac{E}{f}\right)^4 f^2}{p_{in}} - k_{i0n}{}^2 . k_{i0}{}^2} \tag{10}$$

where $kHVF$ is the harmonic voltage factor as defined by NEMA [16]. It was placed in the equation originally conceived as (5) for the influence of the PWM supply voltage harmonics to be also considered on the motor temperature rise. For most of the modern static frequency converters $kHVF$ is 0.95.

As a consequence of the cooling reduction, kT is usually lower than 1. However, if the minimized total losses are such that reduce the motor temperature rise even with poor ventilation, kT can be higher than 1. Similarly, if kT is calculated for an insulation class temperature rise, it will be normally higher than 1 if the rated motor temperature rise is much below the insulation class temperature rise limit.

Fig. 7 presents an example of loss reduction achieved with the proposed method. A three-phase, 30 kW, 4-pole induction motor was tested at constant rated torque within the frequency range from 0.1 to 1.0 (p.u.). The results are presented for three different situations: calculation with constant flux, calculation with optimal flux and testing with optimal flux.

The loss reduction obtained with the proposed technique, as shown in Fig. 7, results in a better thermal performance of the motors operating with optimal flux. Comparing the motor temperature rises when operating at constant flux condition to those when operating at optimal flux condition, it is remarkable a behavior similar to that outlined in Fig. 8, as can be checked in the experimental results presented in section VI.

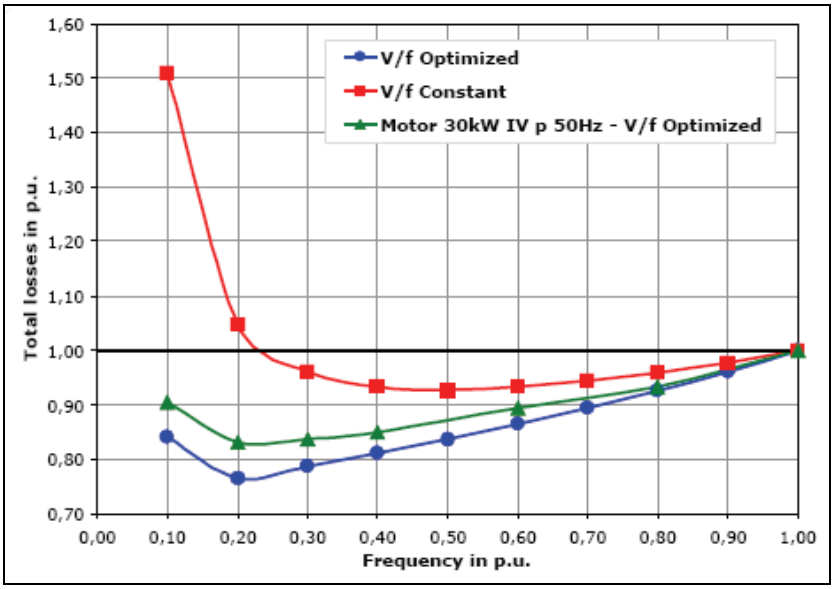

Fig. 7. Total losses (p.u.) x frequency (p.u.)

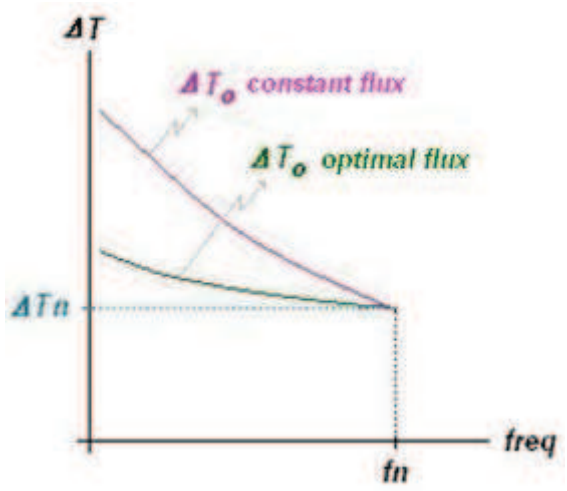

ΔT_n: temperature of thermal stabilization of the motor fed by sinusoidal supply (mains)
ΔT_0: temperature of thermal stabilization of the motor fed by converter supply
fn: operation base frequency of the motor

Fig. 8. Temperature rise x operation frequency, sketch of the motor performance under different flux conditions

5. Validation and implementation of the optimal flux curve

To validate the proposed technique, temperature rise tests with speed/ventilation variation were accomplished for a wide range of industrial motor ratings. This way, it was possible to compare the thermal performances of converter-fed motors when under constant flux (rated losses) and optimal flux (minimum losses) conditions.

Before the implementation of the automatic function for optimal flux selection by the converter, drives with suitably modified softwares were used, so that specific flux values could be manually adjusted. This allowed the practical correction of the curve obtained by means of mathematical calculations and the finding of the actual optimal flux curve that was implemented in the converters used in the tests, into which were incorporated the automatic function for the optimal flux setting.

As the sensorless vector control enables the magnetic flux of the motor to be directly altered, this was the control type employed in all tests with converter. The switching frequency used in all tests with converter was 2.5 kHz.

A. NEMA High Efficiency (NHE) Motors

The motors to be tested were selected considering the worst horsepower/frame size ratios criteria. The following machines were used in the tests, all of them 4-pole (predominant polarity in low-voltage industrial applications) and all of them with class F insulation: 5 hp (NEMA 184T); 20 hp (NEMA 256T); 50 hp (NEMA 326T) and 150 hp (NEMA 444T). Occasionally, for investigation of specific issues, tests were also realized with motors that are not related above.

It should be noted that the loss minimization technique was conceived and developed specifically for low operation frequencies (below 0.5 p.u.). Thus, at base (rated) frequency, in this case 60 Hz, the flux value for the minimum losses condition is the rated flux. The tests were conducted with full load being continuously applied until the motor thermal stabilization.

B. NEMA Premium Efficiency (NPE) Motors

Considering that NEMA Premium Efficiency motors tend to present lower temperature rises than NEMA High Efficiency motors, few NPE motors were tested just for the effectiveness of the proposed loss minimization technique to be corroborated with such motors. Despite that tests were conducted with 2- and 4-pole motors of very distinct horsepower rates, in order to extend the solution also for machines of other polarities. The following motors were tested: 5 hp (NEMA 184T) and 150 hp (NEMA 444T).
The tests were conducted in a way similar to the followed for NHE motors: continuous application of full load until the thermal stabilization of the motor.

C. EFF1 (IE3) Motors

The several motors tested were chosen according to the criterion of the most critical frame size/horsepower ratios. They were all 4-pole machines, since this polarity is typical in low-voltage applications involving speed variation. Motors with base frequencies of both 50 and 60 Hz were tested, for a wider verification of the proposed solution, as listed below:

- f_{base} = 60 Hz: 3 hp (IEC 90L), 12.5 hp (IEC 132M), 50 hp (IEC 200L), 75 hp (IEC 225SM) and 150 hp (IEC 280 SM).

- f_{base} = 50 Hz: 2hp (IEC 90L), 10 hp (IEC 132M), 40 hp (IEC 200L), 75 hp (IEC 225SM) and 150 hp (IEC 280 SM).

Regarding the temperature rise tests, it should be noted that at 50 or 60 Hz the motors were always fed by the mains (AC power line), that is, sinusoidal supply was used, while all the other tests were accomplished with the motors fed by converter in optimal flux condition for loss minimization. Due to the fact that EFF1 (IE3) motors usually present lower efficiency levels than NHE and NPE motors, they tend to operate a little bit warmer than the latter. Because of that, unlike the tests performed with NHE and NPE motors, sometimes derating factors were applied in the tests with EFF1 (IE3) motors at low frequencies. However, in all cases the tests were performed following S1 duty as well.

6. Experimental results

The results contained in Tables I and II evidence the effectiveness of the proposed loss minimization technique for NEMA High Efficiency and NEMA Premium Efficiency motors: all the motors tested with optimal flux got the thermal stabilization at a lower temperature than with constant flux, at all frequencies analysed. Furthermore, Tables I and II show that, when operating at minimum loss condition, NHE and NPE motors can provide the rated torque continually throughout the operation range, even at low frequencies.
Tables I and II present some lacking results of low frequency (typically 5 Hz or below) tests. In these cases, the respective temperature rise test at full load could not be concluded, either because the motor was already running too hot, forcing the interruption of the test before thermal stabilization was reached, or because the dynamometer could no longer apply the

required test load after a period, due to its functioning principle (braking/loading caused by the Foucault effect) and given the increased slip of the motor when it is heated. Temperature rise tests that could not be concluded properly with constant flux, but could be normally performed in the optimal flux condition, are themselves evidences of the thermal performance improvement of the motor, provided by the loss minimization technique.

Source	Operation Frequency	Flux	5 hp	20 hp	50 hp	150 hp
Mains supply	60 Hz sinusoidal	constant	50.3	48.1	53.8	67.7
Converter	60 Hz	constant	51.3	59.1	77.7	86.6
		optimal				
	15 Hz	constant	72.8	79.8	122.3	100.3
		optimal	72.8	62.4	79.8	82.6
	10 Hz	constant	101.0	104.7		125.3
		optimal	77.8	67.7	88.1	83.2
	5 Hz	constant				
		optimal	82.8	80.6	115.8	97.4

Table I. Temperature rise tests results (K) 4-pole nhe motors – s1 duty

Source	Operation Frequency	Flux	5 hp – 4p	150 hp – 4p	5 hp – 2p
Mains supply	60 Hz sinusoidal	constant	28.4	66.5	31.1
Converter	60 Hz	constant	32.5	*	*
		optimal			
	30 Hz	constant	39.9	*	*
		optimal	36.5	*	*
	10 Hz	constant	65.5	*	40.2
		optimal	55.0	*	29.5
	5 Hz	constant		*	
		optimal	67.9	*	82.1
	4 Hz	constant		*	*
		optimal	100.0	*	*
	3 Hz	constant			*
		optimal	*	87.4	*

*Tests that have not been performed

Table II. Temperature rise tests results (K) npe motors – s1 duty

The analysis of the data presented in the tables above by means of graphs makes the interpretation of results easier. Fig. 9 evidences the advantages of using the optimal flux technique with a NHE, 20 hp, 4-pole motor.

Some results of temperature rise tests realized with EFF1 (IE3) motors under optimal flux condition are graphically presented in Figs. 10 to 13.

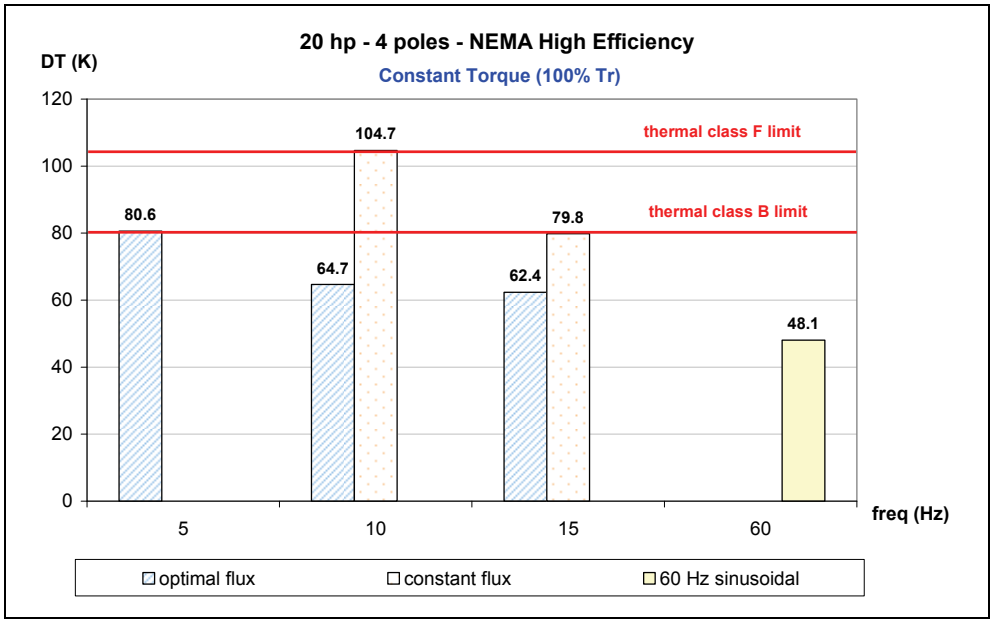

Fig. 9. Examples of results of temperature rise tests accomplished with NHE motor

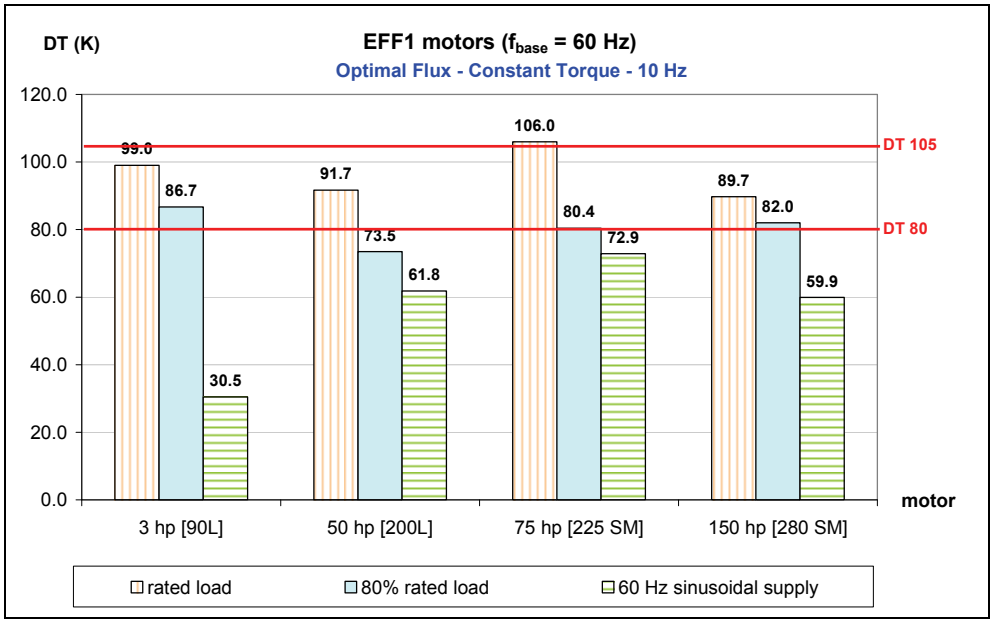

Fig. 10. Results of temperature rise tests conducted with EFF1 (f_{base} = 60 Hz) motors running at 10 Hz

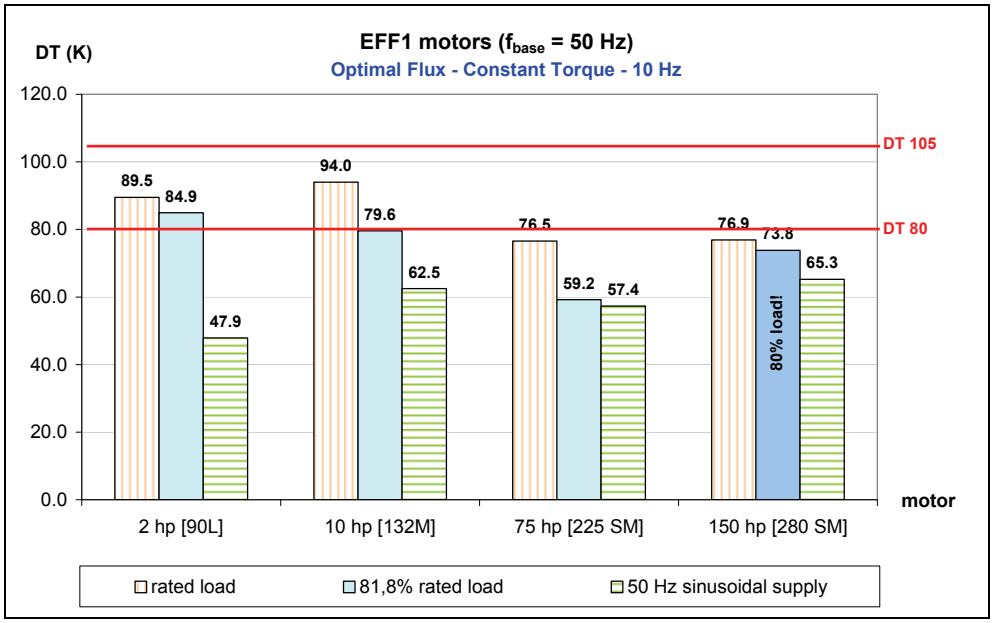

Fig. 11. Results of temperature rise tests conducted with EFF1 (f_{base} = 50 Hz) motors running at 10 Hz

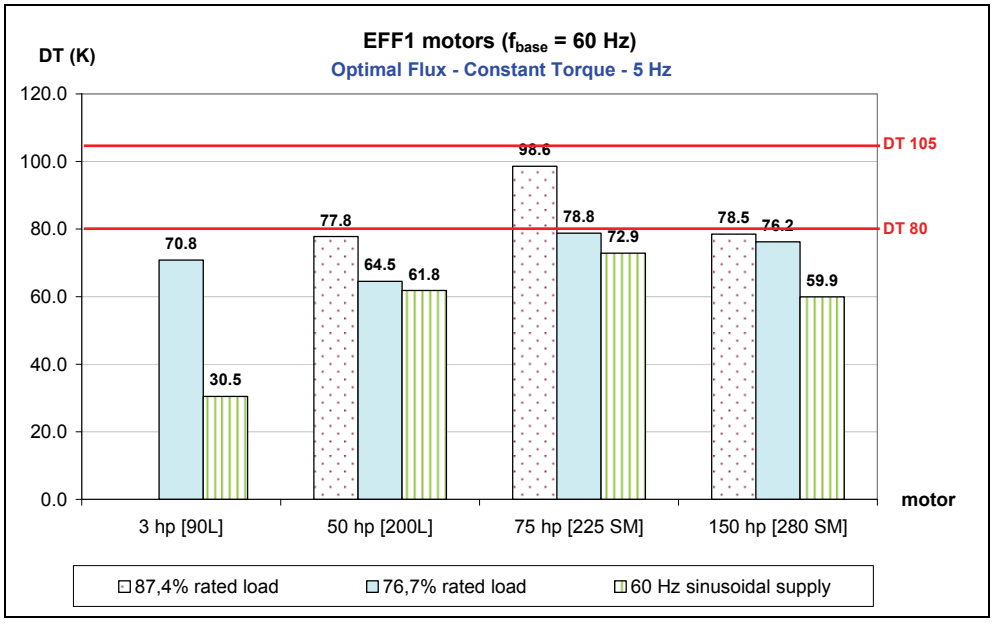

Fig. 12. Results of temperature rise tests conducted with EFF1 (f_{base} = 60 Hz) motors running at 5 Hz

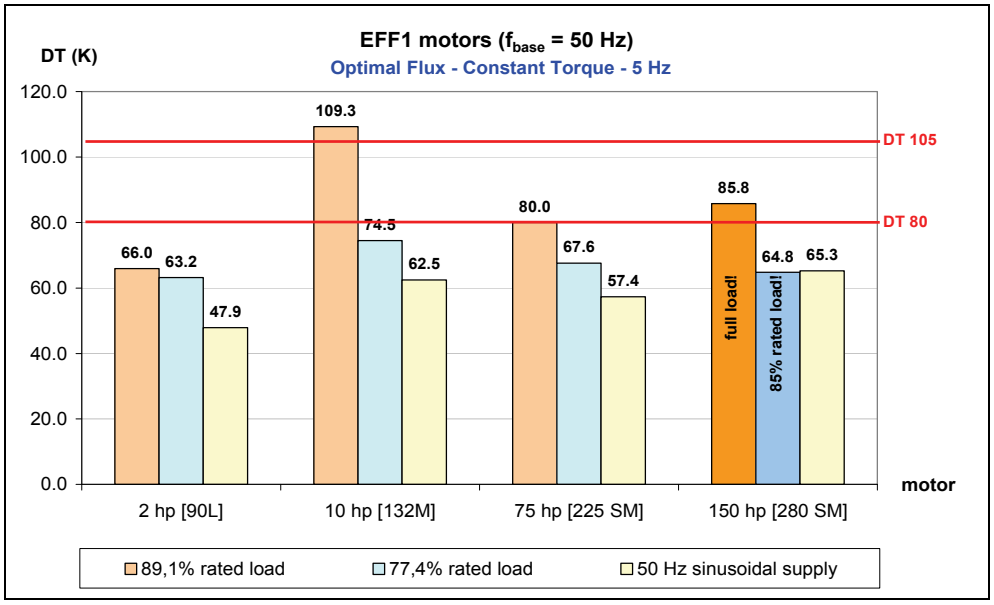

Fig. 13. Results of temperature rise tests conducted with EFF1 (f_{base} = 50 Hz) motors running at 5 Hz

7. Conclusions

The study on the behavior of 3-phase induction low voltage motors' losses as a function of parameters such as load, operation frequency and magnetic induction (flux density), brought about the conception of an equation for magnetic flux that minimizes the total motor losses in each operation frequency. This is very interesting, given that variable speed drives usually involve operation throughout a speed range. Frequency reduction causes the motor iron losses to decrease, thus allowing the magnetic induction (or flux) to be increased at low operation speeds, enabling the motor to provide torque with lower current. The flux increase results from an increment in voltage/frequency ratio, accomplished in a growingly more accentuated manner the lower the operation frequency.

The mathematical equation that has been created was implemented in commercial static frequency converters and the study validation was carried out by means of the analysis of specific motor lines and the execution of tests with a number of frequency converters and induction motors of distinct sizes, using the optimal flux ratios theoretically determined. The tests led to the definition of the actual optimal flux curve as well as new derating curves valid for motors working under optimal flux condition, which evidence the advantages provided by the proposed technique (Fig. 14).

According to Fig. 14, it is possible to note that if temperature rise of thermal class F (105ºC) is permitted on the motor windings, the loss minimization technique prevents the need of torque reduction for operation of the motor at low frequencies (until 0.1 p.u.). If temperature rise of thermal class B (80ºC) is required, the loss minimization technique allows for the application of a smoother torque derating than the needed for the motor running with constant flux and rated losses.

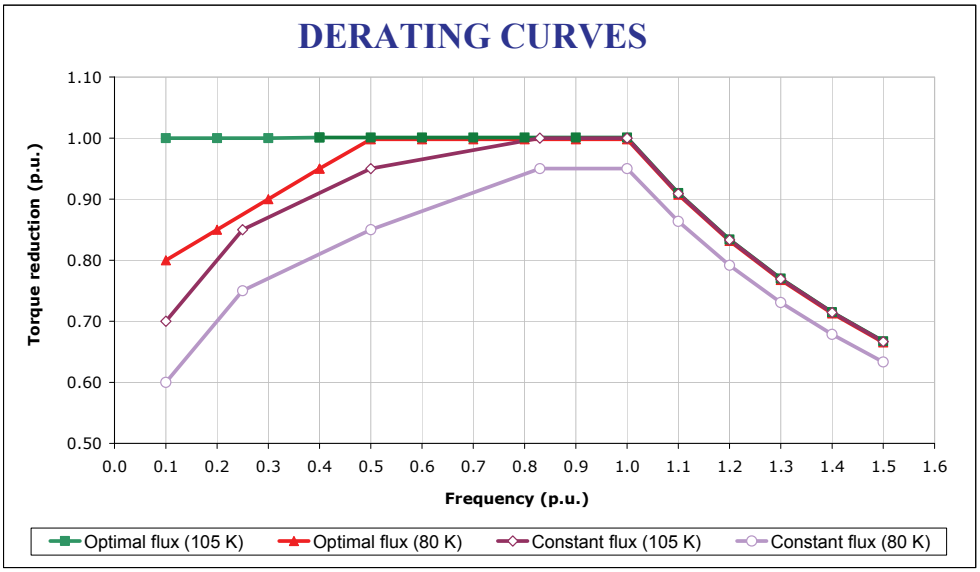

Fig. 14. The new derating (torque reduction) curves proposed evidence the advantages provided by the optimal flux solution

The implementation of the optimal flux curve into commercial frequency converters resulted in the development of a solution (converter + motor) to optimize/improve the variable speed drives with constant torque loads.
The next step of this development (ongoing) is improving the Optimal Flux Solution, so that it can be advantageously used with any type of load driven by converter-fed induction motors.

8. References

[1] PCT/BR2004/000074, "Static frequency converter with automatic function for optimizing magnetic flux and minimizing losses in electric induction motors".
[2] S. L. Nau and A. P. Sobrinho, "Optimal voltage/frequency curve for inverter-fed motor". Proceedings of the 3rd International Conference on Energy Efficiency in Motor Driven Systems (EEMODS), Treviso, Italy, 2002.
[3] R. Kaczmarek; M. Amar and F. Protat, "Iron loss under PWM voltage supply on Epstein frame and in induction motor core". IEEE Transactions on Magnetics, Vol. 32, No.1, January 1996.
[4] A. Boglietti; P. Ferraris; M. Lazzari and F. Profumo, "Iron losses in magnetic materials with six-step and PWM inverter supply". IEEE Transactions on Magnetics, Vol. 27, No. 6, November 1991.
[5] L. T. Mthombeni and P. Pillay, "Core losses in motor laminations exposed to high-frequency or nonsinusoidal excitation". IEEE Transactions on Industry Applications, Vol. 40, No. 5, September-October 2004.

[6] M. S. Lancarotte; C. Goldemberg and A. A. Penteado Jr, "Estimation of FeSi core losses under PWM or DC bias ripple voltage excitations". IEEE Transactions on Energy Conversion, Vol. 20, No. 2, June 2005.

[7] A. J. Moses and N. Tutkun, "Investigation of power loss in wound toroidal cores under PWM excitation". IEEE Transactions on Magnetics, Vol. 33, No. 5, September 1997.

[8] A. Boglietti; M. Chiampi; M. Repetto; O. Bottauscio and D. Chiarabaglio, "Loss separation analysis in ferromagnetic sheets under PWM supply". IEEE Transactions on Magnetics, Vol. 34, No. 4, July 1998.

[9] A. Boglietti; P. Ferraris; M. Lazzari and M. Pastorelli, "About the possibility of defining a standard method for iron loss measurement in soft magnetic materials with inverter supply". IEEE Transactions on Industry Applications, Vo. 33, No. 5, September-October 1997.

[10] C. Cester; A. Kedous-Lebouc and B. Cornut, "Iron loss under practical working conditions of a PWM powered induction motor". IEEE Transactions on Magnetics, Vol. 33, No. 5, September 1997.

[11] A. Ruderman and R. Welch, "Electrical machine PWM loss evaluation basics". Proceedings of the 4th International Conference on Energy Efficiency in Motor Driven Systems (EEMODS), Heidelberg, Germany, 2005.

[12] M. Sokola; V. Vuckovic and E. Levi, "Measurement of iron losses in PWM inverter fed induction machines". Proceedings of the 30th Universities Power Engineering Conference (UPEC), London, UK, 1995.

[13] A. C. Smith and K. Edey, "Influence of manufacturing processes on iron losses". Proceedings of the 7th International Conference on Electrical Machines and Drives - Conference Publication No. 412. September 1995.

[14] K. Kostenko e L. Piotrovski, Máquinas Eléctricas – Volume II – Máquinas de Corrente Alternada (tradução de original russo), Ed. Lopes da Silva, Porto, Portugal, 1979.

[15] P. C. Krause, Analysis of Electric Machinery, McGraw Hill, New York, USA, 1996.

[16] NEMA Standard MG1-2003, Part 30 – Application considerations for constant speed motors used on a sinusoidal bus with harmonic content and general purpose motors used with adjustable-voltage or adjustable-frequency controls or both.

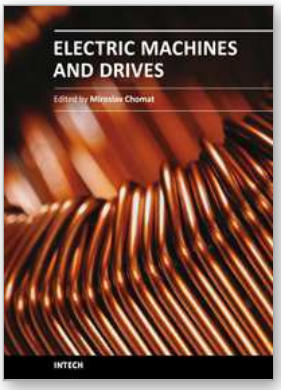

Electric Machines and Drives
Edited by Dr. Miroslav Chomat

ISBN 978-953-307-548-8
Hard cover, 262 pages
Publisher InTech
Published online 28, February, 2011
Published in print edition February, 2011

The subject of this book is an important and diverse field of electric machines and drives. The twelve chapters of the book written by renowned authors, both academics and practitioners, cover a large part of the field of electric machines and drives. Various types of electric machines, including three-phase and single-phase induction machines or doubly fed machines, are addressed. Most of the chapters focus on modern control methods of induction-machine drives, such as vector and direct torque control. Among others, the book addresses sensorless control techniques, modulation strategies, parameter identification, artificial intelligence, operation under harsh or failure conditions, and modelling of electric or magnetic quantities in electric machines. Several chapters give an insight into the problem of minimizing losses in electric machines and increasing the overall energy efficiency of electric drives.

InTech Europe
University Campus STeP Ri
Slavka Krautzeka 83/A
51000 Rijeka, Croatia
Phone: +385 (51) 770 447
Fax: +385 (51) 686 166
www.intechopen.com

InTech China
Unit 405, Office Block, Hotel Equatorial Shanghai
No.65, Yan An Road (West), Shanghai, 200040, China
中国上海市延安西路65号上海国际贵都大饭店办公楼405单元
Phone: +86-21-62489820
Fax: +86-21-62489821